SCIENCE CHINA
Technological Sciences

September 2011 Vol.54 No.9: 2457–2467
doi: 10.1007/ s11431-011-4428-7

Heat transfer blockage in small scale combustion of polymers

JIANG FengHui[1,2*], QI HaiYing[1], J. L. de RIS[2] & M. M. KHAN[2]

[1]*Key Laboratory for Thermal Science and Power Engineering of Ministry of Education, Tsinghua University, Beijing 100084, China;*
[2]*FM Global Engineering & Research, 1151 Boston-Providence Turnpike, P.O. Box 9102, Norwood, MA 02062, USA*

Received January 12, 2011; accepted April 1, 2011; published online June 21, 2011

Flame heat transfer blockage occurs as fuel vapors, soot and products of combustion near a burning fuel surface block much of the heat feedbacks (including external radiative heat flux) to the fuel surface of a burning object. Blockage clearly affects burning rates and heat release rates of fires. This needs to be included when calculating flame heat transfer in fire growth models. An understanding of burning of materials in small scale fires is of broad and vital importance for predicting their burning performance in large scale fires. The blockage phenomenon was clearly observed and quantitatively measured in experiments that took advantage of the unique capability of the Fire Propagation Apparatus (FPA) of being able to vary the ambient oxygen concentrations. An indirect measurement approach was established which provides an experimental understanding of the concept of the blockage. The measurements were further explained by a one-dimensional steady-state model of a diffusion flame, which focuses on the radiant absorption and emission by the gas-soot mixture of flames. The theoretical model provides a greater understanding of the fundamental knowledge of the blockage. The overall heat transfer blockage factor can be up to 0.3 –0.4 for PMMA and POM. The factor and its components are nearly independent of the external radiation, but increase as the ambient oxygen concentration rises. A comparison between experimental data and model prediction shows a good agreement.

polymer, flame heat transfer blockage, gas-soot mixture, gas absorption and emission, external radiant heat flux, oxygen concentration

Citation: Jiang F H, Qi H Y, de Ris J L, et al. Heat transfer blockage in small scale combustion of polymers. Sci China Tech Sci, 2011, 54: 2457–2467, doi: 10.1007/ s11431-011-4428-7

1 Introduction

Flame heat transfer blockage is a fundamental phenomenon in combustion of fires. For a burning object in fires, both external heat sources and the flames provide heat feedbacks to the burning surface for vaporizing. Released fuel vapors therefore mix with air and burn above the surface with flames consisting of gas-soot mixtures including unburned fuel vapors and combustion products. In most cases of fires, the primary heat feedbacks from external heat sources and the flames to the fuel surface are transferred by radiation. Therefore, the question is whether the gas-soot mixture above the fuel surface is "transparent" for the radiative heat feedbacks. It is known that soot and some gases absorb and scatter radiative energy so that radiant heat fluxes are attenuated as they penetrate flames. On the other hand, emission and forward scattering from the gas-soot mixture enhance the thermal radiation as a result of the absorption of external radiation. Which, among the two effects, i.e. attenuation and enhancement, is stronger? or are they always equally powerful? In addition, how are the effects further enhanced by mass transfer of cool pyrolysis gases leaving a burning fuel surface and convecting heat away from the surface?

Flame heat feedbacks are critical in predicting fire burning rates and heat release rates, which are the key parameters in determining how fast fires would grow and propagate. In order to accurately model fire growth and propagation,

*Corresponding author (email: jiang.fenghui@fmglobal.com)

understanding and prediction of flame heat transfer need to be improved by including the blockage effect [1−3]. Lack of knowledge of flame heat transfer blockage affects the accuracy of fire growth models. Therefore, conceptual and quantitative answers to the above questions are of broad importance in improving the understanding of flame heat transfers, increasing accuracy of theoretical fire models, as well as developing material flammability/combustibility test and approval techniques.

In most previous and present researches on fire growth models and relevant developments, the flame heat transfer blockage effects were ignored [4−6]. At present, research on this fundamental problem has become a "bottleneck" [7] with increased demands for material flammability testing technique and rapid development of theoretical fire growth models. Therefore, it is necessary and crucial to conduct a fundamental research specifically for this key problem in order to extend the knowledge for developing material flammability testing technique and methodology.

Flame heat transfer blockage is a relatively new area of attention in the field of flame radiation researches. To date, knowledge development regarding this phenomenon has experienced two main phases, the first phase was phenomenon observations and the second is preliminary studies. In 1970s and 1980s, heat transfer blockage was observed in a lot of combustion phenomena related to fire hazard, such as compartment fires [8], pool fires [9] and soot mantle [10] etc. In the second phase, more progresses had been shown in experiments and theoretical analysis within the recent two decades, it was found that as much as 40% of the radiation directed toward a fuel surface could be blocked by the cool sooty gases near the fuel surface [11, 12]. However, currently understanding of the flame heat transfer blockage effects is still quite limited, the underlying knowledge is scattered rather widely in literature. Some recent representative research includes:

(1) Experimental studies and data accumulations, such as an experimental study of radiative heat feedback and blockage on vertical wall fires [13], measurements on absorptivity and emissivity of fuel vapors [14, 15], various models on soot formation, transfer and consumption within flames as well as soot radiation [16−20], measurements of heat of gasification/vaporization for small scale polymer samples [21, 22] and experimental simulation and measurement on radiative heat feedbacks using gas flames [23] etc.

(2) Simplified theoretical models, such as a one-dimensional model on radiative blockage by soot layer within a flame [24], a compartment fire model that includes the effects of radiation blockage [25] and a dimensionless model on the blockage of flame heat transfer by a cool soot layer surrounding a cold object immersed in a large flame volume [26, 27] etc. Although these simplified theoretical models are considered preliminary focusing only on isolated problems, they were quite helpful to extending knowledge and creating continuous interest in the heat transfer blockage phenomena.

(3) Numerical and analytical studies, such as Baek et al. [28] and Chen et al. [29] solved one-dimensional equations of energy conservation and radiative heat fluxes with constant properties, under the assumption that soot particles dominate the absorbing-emitting process, the influence of temperature and optical thickness profiles on flame heat transfer blockages was evaluated; Bedir et al. [30] completed a numerical study on PMMA diffusion flames with flame radiation in a stagnation-point geometry, a narrow-band radiation model was used to evaluate the absorption and emission from CO_2, water vapor and MMA (fuel) vapor, and the net radiative heat flux was given as a function of the flame stretch rate, contributions from these three species to the emission at different stretch rates were investigated and compared. Overall the above numerical studies had made great contributions in revealing and explaining the physical nature and internal link of the phenomena, although they lacked of experimental support and might have space for further improvement in integrity and systematicness.

With the great progresses in the two phases, a certain knowledge of heat transfer blockages, such as that about the causes, mechanism and magnitude, has been obtained and accumulated. However, some deficits may still exist in the previous researches. In terms of content, previous researches concentrated more on soot absorption and emission, with ignoring gases as participating species. A main reason for this was that gas radiation is more difficult to handle. In terms of approach, theoretical and experimental studies are somehow isolated, because direct measurements of heat transfer blockage are difficult, so that not many commonly accepted experimental methods are available at present and development of experimental methodology and measurement technique still need to be strengthened. In terms of integrity of knowledge, understanding of the flame heat transfer blockage phenomenon is still incomplete and limited.

As a fundamental research, the purpose of this study is to experimentally and theoretically extend the conceptual and quantitative understanding of the flame heat transfer blockage phenomenon. In the experimental study, taking advantage of the unique capabilities of the Fire Propagation Apparatus (FPA), an experimental approach of indirect measurement of heat transfer blockage was developed, and accurate experimental data was obtained. In the physical model study, based on the theories of combustion and heat transfers, a one-dimensional steady-state model of diffusion flame was developed focusing on absorption and emission by the gas-soot mixture above the fuel surface as demonstrated in the experiments. The processes of heat and mass transfers within the flames were analyzed in detail for understanding the mechanism and effects of the heat transfer blockage. In the mathematical model study, simultaneous

equations for energy conservation, radiance and radiative heat fluxes were numerically solved. A mathematical technique for conveniently solving flame heat transfer problems was established. Specific accomplishments of this study are summarized as follows:

(1) Establishing an "approximate band model" for fuel vapors and inserting it into RADCAL to compute radiances from inhomogeneous flames;

(2) Extending the concept of a one-dimensional model of diffusion flames to variable properties, as well as the absorption and emission by gas-soot mixture;

(3) Extending application of one-dimensional flame model to conical flames and studying effects of the external heat flux and ambient oxygen concentration on flame heat transfer and burning rate.

Combination of experimental and theoretical efforts is an additional unique feature of this study. In previous researches, examples having both experiments and theoretical model that provide identical and complementary results were still rare. The approaches of this study were to prove and study the phenomena and collect the accurately measured data by experiments, develop an independent theoretical model and verify it by various experimental data, and finally use the verified model to carry out more detailed and extensive researches.

2 Definition and measurement of flame heat transfer blockage

The experimental study was performed in FPA in the Flammability Laboratory of FM Global Research, Norwood, MA, USA. FPA is the widely utilized research equipment in evaluating and characterizing material fire properties as related to fire hazards under simulated full-scale fire conditions, and ASTM E-2058 was adopted.

Two different black polymers, polymethylmethacrylate (PMMA) and polyoxymethylene (POM) were selected as burning samples in this study. Mass loss rates were measured when samples were pyrolyzed in a pure nitrogen atmosphere and also burnt in air with 18%, 30% and 40% ambient oxygen-nitrogen, respectively, while being subjected to various external radiant fluxes. Some of the experimental results were already reported in the previous paper [31].

It was observed in the experiments that: (1) With the external radiant fluxes ranging from 0 to 60 kW/m^2, typically, mass loss rates have a linear dependence on the external radiant heat fluxes. (2) For PMMA samples, a certain amount of soot exists within flames, and soot generation is sensitive to variations of the ambient oxygen concentration; while for POM samples, there is no visible soot within flames, flames are completely transparent. This indicates that a portion or the whole of flame radiation is emitted from gases, therefore gas radiation should not be neglected in flame radiation evaluations. Based on this observation, in the subsequent theoretical model, more efforts focus on absorption and emission by gases, especially the fuel vapors.

2.1 Heat of gasification

Determination of an accurate heat of gasification for the burning samples is important in experimentally evaluating heat transfer blockage. As a sample is pyrolyzed in a pure nitrogen atmosphere, energy balance on the surface can be written as

$$\dot{q}''_{\text{ext}} - \dot{q}''_{\text{loss}} = \dot{m}''_{\text{p}} \Delta H_{\text{g}} \tag{1}$$

where $\dot{m}''_{\text{p}}$ is the pyrolysis mass loss rate (pyrolysis rate); ΔH_{g} is the heat of gasification (kJ/g); $\dot{q}''_{\text{ext}}$ is the external radiant heat flux, and $\dot{q}''_{\text{loss}}$ is a surface heat loss (mainly surface re-radiation). Using ΔH_{g} as a divisor on both sides of eq. (1), it is derived that

$$\dot{m}''_{\text{p}} = \frac{1}{\Delta H_{\text{g}}} \dot{q}''_{\text{ext}} - \frac{\dot{q}''_{\text{loss}}}{\Delta H_{\text{g}}}. \tag{2}$$

This linear function was obtained in experiments, measuring the pyrolysis rate $\dot{m}''_{\text{p}}$ while varying the external radiant flux. The inverse of the slope k_{p} is the heat of gasification, i.e.

$$\Delta H_{\text{g}} = 1 / k_{\text{p}}. \tag{3}$$

The linear function further confirmed that the heat of gasification is a material property, independent of external heat fluxes.

2.2 Heat transfer blockage factors

On a burning surface, when an incident radiant heat flux $\dot{q}''_{\text{ext}}$ penetrates the flame, it is attenuated by the mixture of gases and soot within flames due to the absorption and scattering effect, with a residue heat flux $\dot{q}''_{\text{es}}$ arriving at the surface. Thus β_{ext} is defined as a blockage factor for the external radiation. i.e.

$$\beta_{\text{ext}} = \frac{\dot{q}''_{\text{ext}} - \dot{q}''_{\text{es}}}{\dot{q}''_{\text{ext}}} = 1 - \frac{\dot{q}''_{\text{es}}}{\dot{q}''_{\text{ext}}}, \tag{4}$$

which is the fraction of external radiation that is absorbed by the flames and does not reach the surface as it penetrates the flames.

Meantime, due to the involvement of the external radiation, the gas-soot mixture within flames is heated as a result of thermal absorption, flame heat feedback to the surface therefore varies in contrast to the circumstance without the external radiation. Thus β_{int} is defined as a blockage factor for flame heat feedback itself, i.e.

$$\beta_{\text{int}} = \frac{\dot{q}''_{\text{f-net}}\big|_0 - \dot{q}''_{\text{f-net}}}{\dot{q}''_{\text{ext}}}. \quad (5)$$

Here $\dot{q}''_{\text{f-net}}\big|_0$ is the net "free burn" heat feedback from the flames to the surface with $\dot{q}''_{\text{ext}} = 0$. It includes the radiative and convective heat transfer from the flames minus the surface heat loss. While $\dot{q}''_{\text{f-net}}$ is the net flame heat feedback in the presence of the external radiation. A fraction of external radiation absorbed by the flames heats the flames causing them to emit additional radiation. Therefore, $\dot{q}''_{\text{f-net}}$ includes (1) the increased radiative heat transfer from the flames, (2) the convective heat transfer which is now reduced because of the increased mass transfer, and (3) minus the surface heat loss.

With the assumption that all net heat fluxes arriving at the fuel surface are absorbed by the fuel for gasification, the following heat balance exists at the burning surface:

$$\dot{q}''_{\text{es}} + \dot{q}''_{\text{f-net}} = \dot{m}''\Delta H_{\text{g}}. \quad (6)$$

Solving eqs. (4) and (5) for $\dot{q}''_{\text{es}}$ and $\dot{q}''_{\text{f-net}}$ respectively, and substituting them into eq. (6), the mass burning rate can be derived as

$$\dot{m}'' = \frac{(1-\beta_{\text{ext}}-\beta_{\text{int}})}{\Delta H_{\text{g}}}\dot{q}''_{\text{ext}} + \frac{\dot{q}''_{\text{f-net}}\big|_0}{\Delta H_{\text{g}}} = k_{\text{b}}\dot{q}''_{\text{ext}} + \dot{m}''_{\text{b}}. \quad (7)$$

In the linear relationship between $\dot{m}''$ and $\dot{q}''_{\text{ext}}$ $\dot{m}''_{\text{b}}$ represents a "free burning" rate in any ambient oxygen concentration without external radiation. With eq. (3), the overall heat transfer blockage factor β can be derived by equating the slopes (k_{b}) of the above linear function, i.e.

$$\beta = \beta_{\text{ext}} + \beta_{\text{int}} = \frac{\dot{q}''_{\text{ext}} + \dot{q}''_{\text{f-net}}\big|_0 - (\dot{q}''_{\text{es}} + \dot{q}''_{\text{f-net}})}{\dot{q}''_{\text{ext}}} = 1 - k_{\text{b}}/k_{\text{p}}. \quad (8)$$

Here in the numerator $\dot{q}''_{\text{ext}} + \dot{q}''_{\text{f-net}}\big|_0$ represents the total heat flux "paid" to the burning surface including the external radiant flux; while $\dot{q}''_{\text{es}} + \dot{q}''_{\text{f-net}}$ represents the "residue" heat feedbacks "received" by the burning surface under the same circumstance. The difference between "paid" and "received" is the loss of energy. Therefore, β represents the fraction of total heat feedback energy loss related to external radiation.

Eq. (8) not only defines the blockage factor of heat feedbacks to the burning surface β, but also establishes a "bridge" between theoretical predictions and experimental measurements. On the right hand side, the ratio of the slopes, i.e. the slope of "burning lines" of various ambient oxygen concentrations k_{b} and the slope of the "pyrolysis line" of zero ambient oxygen concentration k_{p}, can be determined by experiments. On the left hand side, the various heat fluxes can be computed by a theoretical model. This simple equation inherently as well as experimentally describes heat transfer blockage, and lays a foundation for comparisons between model predictions and experimental measurements.

Additionally, in eq. (8), the net flame heat feedbacks to the burning surface have radiative and convective components, i.e.

Without external radition:

$$\dot{q}''_{\text{f-net}}\big|_0 = \dot{q}''_{\text{rads}}\big|_0 + \dot{q}''_{\text{cons}}\big|_0 - \dot{q}''_{\text{loss}}. \quad (9)$$

With external radiation

$$\dot{q}''_{\text{f-net}} = \dot{q}''_{\text{rads}} + \dot{q}''_{\text{cons}} - \dot{q}''_{\text{loss}}. \quad (10)$$

Here the subscripts, rad, con and s, mean radiative, convective and surface respectively. Assuming the burning surfaces are nearly a black surface, $\dot{q}''_{\text{loss}}$ is almost independent of external radiative intensities. Substituting eqs. (9) and (10) into eq. (8), the overall blockage factor can be written as

$$\beta = \frac{(\dot{q}''_{\text{ext}} - \dot{q}''_{\text{es}}) + (\dot{q}''_{\text{rads}}\big|_0 - \dot{q}''_{\text{rads}}) + (\dot{q}''_{\text{cons}}\big|_0 - \dot{q}''_{\text{cons}})}{\dot{q}''_{\text{ext}}} = \beta_{\text{rad}} + \beta_{\text{con}}, \quad (11)$$

giving:

$$\beta_{\text{rad}} = \frac{(\dot{q}''_{\text{ext}} - \dot{q}''_{\text{es}}) + (\dot{q}''_{\text{rads}}\big|_0 - \dot{q}''_{\text{rads}})}{\dot{q}''_{\text{ext}}}, \quad (12)$$

$$\beta_{\text{con}} = \frac{(\dot{q}''_{\text{cons}}\big|_0 - \dot{q}''_{\text{cons}})}{\dot{q}''_{\text{ext}}}. \quad (13)$$

Eqs. (11)–(13) demonstrate that the overall heat transfer blockage factor also has its radiative and convective components, defined as the radiative blockage factor and convective blockage factor respectively. The former represents a sum of attenuation of external radiation and reinforcement of net flame radiative heat feedback ($\dot{q}''_{\text{rads}} > \dot{q}''_{\text{rads}}\big|_0$); the latter represents the reduced flame convective heat feedback ($\dot{q}''_{\text{cons}} < \dot{q}''_{\text{cons}}\big|_0$) as a result of the increased mass transfer at the burning surface. $\beta_{\text{rad}} \approx 0$ would imply that flames are almost "transparent" for thermal radiation.

The overall heat transfer blockage factor can be measured from experiments based on eq. (8), however, its components β_{ext}, β_{int}, β_{rad} and β_{con} can only be obtained from a theoretical model at present. This displays the unique advantage in the approach of this study to extend understandings and quantify heat transfer blockage by both experiments and an experimentally verified theoretical model.

3 Theoretical model

3.1 One-dimensional steady-state diffusion flame model description and assumption

Focusing on absorption and emission by the gas-soot mix-

ture within flames above the fuel surface, a one-dimensional steady-state model of diffusion flame is developed as illustrated in Figure 1.

An infinite fuel surface at temperature T_s is located at x = 0. As a result of fuel gasification driven by heat feedback to the fuel surface, fuel vapor is released at a constant mass flux, $\dot{m}''$. On the opposite side, the ambient temperature T_{amb} and oxygen concentration $Y_{o\infty}$ are maintained at a screen $x = d$. Oxygen and fuel vapors diffuse toward a flame located between the fuel surface and screen. The infinitely thin flame sheet, having temperature, T_f, divides the entire space into two zones: fuel zone and oxidant zone. The fuel-rich zone contains a mixture of fuel vapor, nitrogen and combustion products (CO_2, H_2O, soot) that diffuse but do not make reaction due to lack of oxygen. The chemical reactions are sufficiently fast to consume all oxygen and most of the fuel at the infinitely thin flame sheet. Owing to incomplete combustion, a very small amount of unburned fuel gas bypasses the flame, performing as an "inert" gas, diffuses through the oxidant zone and is released at the screen. Soot particles are generated at the flame and transported into the oxidant zone where they are partially oxidized. The amount of soot eventually released at the screen is set equal to the experimentally measured smoke yield. For simplicity, it is assumed that the soot retains the same chemical composition of the original fuel. In summary, the oxidant zone contains a mixture of oxygen, nitrogen, combustion products (CO_2, H_2O, soot) and "inert" fuel gas. Oxidization of soot is the only chemical reaction occurring within the oxidant zone. The screen carries away all the heat and combustion products generated by the flame, as well as any unburned "inert" fuel gas and "residual" soot.

The external (incident) radiant flux, $\dot{q}''_{ext}$ is attenuated due to the gradual absorption and scattering by gas-soot mixture within the flames as it passes through the flame, with a "residual" heat flux $\dot{q}''_{es}$ arriving at the fuel surface.

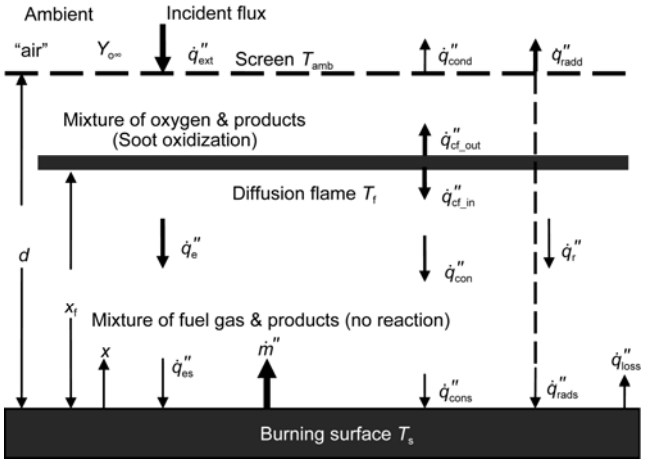

Figure 1 One-dimensional steady-state diffusion flame model.

The flames both emit and absorb radiation. Thermal absorption and emission from the gas-soot mixture within flames are treated separately from the external radiation. The net flame radiation $\dot{q}''_r = \dot{q}''^{+}_r - \dot{q}''^{-}_r$ has both inward (to fuel surface) $\dot{q}''^{+}_r$ and outward (to ambient interface) $\dot{q}''^{-}_r$ components. The inward flame radiation incident on the surface is $\dot{q}''_{rads} = \dot{q}''^{+}_r(0)$. The outward radiant flux emitted by the fuel surface is $\dot{q}''_{loss} = \dot{q}''^{-}_r(0)$ including surface re-radiation and reflection of incident heat fluxes. Therefore, the net (non-external) radiative heat flux at the surface is $\dot{q}''_{rads} - \dot{q}''_{loss}$ assuming the fuel surface is Lambertian with unit emissivity ($\varepsilon_s = 1$). The flame radiation released to the ambient interface is $\dot{q}''_{radd} = \dot{q}''^{-}_r(d)$.

The highest temperature occurs at the flame sheet. As a result of nonuniform profiles of temperature and properties, heat is conducted away from the flame both inward toward the fuel surface and outward toward the ambient interface, eventually reaching the fuel surface with a flux, $\dot{q}''_{cons}$ and the screen with a flux, $\dot{q}''_{cond}$, respectively. Simultaneously the mass transfer coming from the surface convects heat away from the surface toward the ambient interface.

In the experiment, yields of carbon monoxide (CO) and carbon dioxide (CO_2) released from flames were measured. While in this theoretical model, no CO generation in the chemical reactions is assumed for simplicity of the chemistry and mathematics. Actually, the experiment and previous studies have found that generation of CO is much less comparing with generation of CO_2 in most combustion reactions, especially when the ambient oxygen concentration is high. This finding makes this assumption acceptable. Additionally, ideal gas performance is assumed for the gas mixtures involved.

3.2 Model equations

The one-dimensional steady-state diffusion flame model established involves chemical reactions and physical processes of heat and mass transfers. Focusing on the coupled external radiation and flame radiation, its primary objective is to determine the profiles of temperature, species and optical thicknesses etc. in the entire space across the flame. Radiant heat fluxes depend on distributions of the temperature and optical thicknesses. Therefore, the basic mathematical model describing the physics problem is actually to solve the temperature profile from the one-dimensional simultaneous equations of radiance, radiant heat fluxes and energy conservation.

3.2.1 Energy conservation

The transfer of energy from and within a burning environment is controlled by diffusive, convective and radiative

processes. The convection and conduction are coupled to the heating of the flame by radiation, so that a one-dimensional steady-state energy conservation equation can be written as follows for the entire space across the flame:

$$\dot{m}''\frac{\mathrm{d}h_{\mathrm{T}}}{\mathrm{d}x}=\frac{\mathrm{d}}{\mathrm{d}x}\left(\frac{k}{c_{\mathrm{p}}}\frac{\mathrm{d}h_{\mathrm{T}}}{\mathrm{d}x}\right)+\frac{\mathrm{d}\dot{q}_{\mathrm{R}}''}{\mathrm{d}x}, \tag{14}$$

where k and c_{p} are respectively the thermal conductivity and specific heat of the gas mixture. They both vary as a function of temperature and location. The total enthalpy varies smoothly across the flame where sensible enthalpy h_{s} is generated by the release of chemical enthalpy h^0. The total enthalpy is expressed as the sum of the sensible enthalpy and chemical enthalpy, i.e.

$$h_{\mathrm{T}}(x,T)=h_{\mathrm{s}}(x,T)+h^0(x). \tag{15}$$

It remains to evaluate the total radiative heat flux $\dot{q}_{\mathrm{R}}''$ and its spatial derivative which gives a source of heat in the equation. Having all fluxes defined as positive towards the fuel surface and negative towards the ambient interface, the total radiative heat flux is the sum of the external radiant flux $\dot{q}_{\mathrm{e}}''$ and flame radiant flux $\dot{q}_{\mathrm{r}}''$, i.e.

$$\dot{q}_{\mathrm{R}}''(x,T)=\dot{q}_{\mathrm{r}}''(x,T)+\dot{q}_{\mathrm{e}}''(x,T). \tag{16}$$

Evaluation of $\dot{q}_{\mathrm{R}}''$ is here included in a typical one-dimensional steady-state theoretical model of diffusion flames which contains the effects of variable thermal properties. Two transformation variables are introduced such as (1) Z defined as the fraction of original (or supplied) fuel in the mixture and (2) $\eta(x)=\dot{m}''\int_0^x\frac{\mathrm{d}x}{\rho\ \mathrm{D}}=\dot{m}''\int_0^x\frac{c_{\mathrm{p}}}{k}\mathrm{d}x$ defined as a dimensionless mass transfer variable, which simplifies the mathematics. As a result, one-dimensional distributions of species concentrations and thermal properties can easily be solved from the species conservation equations based on the chemical reaction equations established.

3.2.2 *Absorptivity and emissivity of flames*

The absorptivity and emissivity of flames are critical for evaluating the radiative heat flux $\dot{q}_{\mathrm{R}}''(x,T)$ in the energy conservation eq. (14). Flames are treated as mixtures of gases and soot. Accurate evaluation on gas absorption and emission is the key as well as the difficult point in this model development, especially for fuel vapors. As the prophase work of this theoretical model, previous paper [31] provides details of the study and prediction of the absorptivity and emissivity of gas-soot mixtures. For properly handling wavelength dependence of the fuel vapor, an approximate band model was developed and inserted into the RADCAL program, which is based on the statistical narrow band model, to compute radiances from mixtures of the gases. Finally, Curtis-Godson approximation was used to extend the Goody statistical model and evaluate the overall optical thicknesses for inhomogeneous mixtures of gases. For absorption and emission from soot, optical thicknesses were also obtained based on the experimental data of other studies [32] under the grey-body assumption.

3.2.3 *Radiances and radiant heat fluxes*

(1) Outward radiant heat flux

For a volume of gas-soot mixture with given temperature profile $T(x)$ and optical thickness profile $\xi(x)$, the outward radiance can be described by the following universal equation and boundary conditions [33]:

$$\begin{cases}\mu\dfrac{\mathrm{d}I^+}{\mathrm{d}\xi}+I^+=\dfrac{\sigma\ T^4}{\pi}\\ I^+(x=0,\mu)=\dfrac{\dot{q}_{\mathrm{loss}}''}{\pi}\end{cases} \tag{17}$$

Here $\mu=\cos\theta$, and θ is the angle between the ray and the normal. The fuel surface is assumed to be a Lambert surface. $\dot{q}_{\mathrm{loss}}''$ is the radiant heat flux leaving the fuel surface. $\dot{q}_{\mathrm{loss}}''/\pi$ is the radiance in the direction of θ at the fuel surface. The temperature profile $T(x)$ is finally solved from the energy conservation equation, and the optical thickness profile can be computed from eq. (27) of ref. [31].

Solving this differential equation with the boundary condition, the outward radiance is derived as

$$I^+(\xi,\mu)=\frac{\dot{q}_{\mathrm{loss}}''}{\pi}\mathrm{e}^{-\xi/\mu}+\int_0^{\xi/\mu}\frac{\sigma\ T^4}{\pi}\mathrm{e}^{-(\xi-\xi')/\mu}\mathrm{d}\left(\frac{\xi'}{\mu}\right). \tag{18}$$

The radiance in the direction of θ at position ξ/μ consists of two terms. The first term means the residual radiance at ξ/μ as a result of attenuation of the "incident" initial radiance $\dot{q}_{\mathrm{loss}}''/\pi$ as the ray passes an optical thickness of ξ/μ along the θ direction. The second term expresses the accumulated residual radiance at ξ/μ as a result of attenuation of each radiance emitted at ξ/μ from gas-soot mixture of optically thick $(\xi-\xi')/\mu$ as the ray passes an optical thickness of ξ/μ along the θ direction, within the entire optical thickness of ξ/μ in the direction of θ. Therefore, the outward radiant flux can be obtained by integrating the radiance of all rays as θ from $-\pi/2$ to $\pi/2$, i.e.

$$\begin{aligned}\dot{q}_{\mathrm{r\_out}}''(\xi)&=-2\pi\int_0^1 I^+(\xi,\mu)\mu\mathrm{d}\mu\\&=-2\dot{q}_{\mathrm{loss}}''\int_0^1\mu\mathrm{e}^{-\xi/\mu}\mathrm{d}\mu-2\int_0^{\xi}\sigma\ T^4\left[\int_0^1\mathrm{e}^{-(\xi-\xi')/\mu}\mathrm{d}\mu\right]\mathrm{d}\xi'\end{aligned} \tag{19}$$

As the inward direction (toward the fuel surface) is defined as positive, the heat flux in the outward direction

(leaving the fuel surface) is therefore negative. So it is derived that

$$\dot{q}''_{\mathrm{r\_out}}(\xi) = -2\dot{q}''_{\mathrm{loss}}E_3(\xi) - 2\int_0^{\xi}\sigma\ T^4(\xi')E_2(\xi-\xi')\mathrm{d}\xi' \quad (20)$$

Here E_2 and E_3 are the second and third exponential integral functions respectively. The exponential kernel approximation is commonly used for simplicity in radiative transfer problems involving the exponential integral functions.

At the fuel surface, x = 0 and $\xi(0)$ = 0, therefore $\dot{q}''_{\mathrm{r\_out}}(0) = -\dot{q}''_{\mathrm{loss}}$, where $\dot{q}''_{\mathrm{loss}}$ is the radiative heat flux leaving the fuel surface and can be written as

$$\dot{q}''_{\mathrm{loss}} = \varepsilon_s\sigma\ T_s^4 + (1-\varepsilon_s)(\dot{q}''_{\mathrm{rads}} + \dot{q}''_{\mathrm{es}}). \quad (21)$$

Here the first term on the right side is the re-radiation from the fuel surface. $(\dot{q}''_{\mathrm{rads}} + \dot{q}''_{\mathrm{es}})$ is the incident radiant heat fluxes at the fuel surface from the external radiator and the gas-soot mixture within the flames. If ε_s = 1, $\dot{q}''_{\mathrm{loss}}$ becomes only the re-radiation from the fuel surface while ignoring any surface reflection of incident radiant fluxes. In this study, an assumption of ε_s = 1 is employed for simplicity, which is supported by the consistency of the experimental data $\dot{q}''_{\mathrm{loss}}$ and T_s.

At the screen ($x = d$) the outward radiative heat release rate is obtained by setting $\xi = \xi_d$:

$$\dot{q}''_{\mathrm{radd}} = \dot{q}''_{\mathrm{r\_out}}(\xi_d)$$

$$= 2\dot{q}''_{\mathrm{loss}}E_3(\xi_d) + 2\int_0^{\xi_d}\sigma\ T^4(\xi')E_2(\xi_d-\xi')\mathrm{d}\xi' \quad (22)$$

(2) Inward radiant heat flux

Let $y = d - x$, similarly, the inward radiance can be described by the following universal equation and boundary condition:

$$\begin{cases}\mu\dfrac{\mathrm{d}I^-}{\mathrm{d}\zeta} + I^- = \dfrac{\sigma T^4}{\pi} \\ I^-(y=0,\mu) = 0\end{cases} \quad (23)$$

Here the inward optical thickness profile $\zeta(y)$ can be computed from eq. (28) of ref. [31]. Therefore, the inward radiance can be solved as

$$I^-(\zeta,\mu) = \int_0^{\zeta/\mu}\frac{\sigma T^4}{\pi}\mathrm{e}^{-(\zeta-\zeta')/\mu}\mathrm{d}\left(\frac{\zeta'}{\mu}\right). \quad (24)$$

This equation reveals that the radiance at position ζ/μ along the θ direction is generated only by emission from gas-soot mixture within flames, which is the accumulated residual radiance at ζ/μ as a result of attenuation of each radiance emitted at ζ'/μ from the gas-soot mixture of optically thick $(\zeta-\zeta')/\mu$ as the ray passes an optical thickness of ζ'/μ along the θ direction, within the entire optical thickness of ζ/μ in the direction of θ. Similarly, the inward heat flux can be derived as follows by integrating the radiance of all rays (as θ from $-\pi/2$ to $\pi/2$):

$$\dot{q}''_{\mathrm{r\_in}}(\zeta) = 2\pi\int_0^1 I^-(\zeta,\mu)\mu\mathrm{d}\mu$$

$$= 2\int_0^{\zeta}\sigma\ T^4\left[\int_0^1\mathrm{e}^{-(\zeta-\zeta')/\mu}\mathrm{d}\mu\right]\mathrm{d}\zeta' = 2\int_0^{\zeta}\sigma\ T^4(\zeta')E_2(\zeta-\zeta')\mathrm{d}\zeta'. \quad (25)$$

Furthermore, the incident radiant heat fluxes at the fuel surface from the gas-soot mixture can be obtained by letting $\zeta = \zeta_d$ in eq. (25), i.e.

$$\dot{q}''_{\mathrm{rads}} = \dot{q}''_{\mathrm{r\_in}}(\zeta_d) = 2\int_0^{\zeta_d}\sigma\ T^4(\zeta')E_2(\zeta_d-\zeta')\mathrm{d}\zeta'. \quad (26)$$

Consequently, the one-dimensional profile of the net flame radiant flux is derived by combining eqs. (20) and (25):

$$\dot{q}''_{\mathrm{r}}(x) = \dot{q}''_{\mathrm{r\_in}}(\zeta) - \dot{q}''_{\mathrm{r\_out}}(\xi). \quad (27)$$

At the screen, $x = d$ (y = 0), $\zeta(y = 0) = 0$ and $\xi(x = d) = \xi_d$. With eq. (22) the radiative heat released to the ambient interface at the screen can be obtained as

$$\dot{q}''_{\mathrm{r}}(x = d) = -\dot{q}''_{\mathrm{radd}}. \quad (28)$$

While at the fuel surface, x = 0 ($y = d$), $\zeta(y = d) = \zeta_d$ and $\xi(x = 0) = 0$, thus the net heat feedback to the fuel surface from the flame interior is derived as

$$\dot{q}''_{\mathrm{r}}(x = 0) = \dot{q}''_{\mathrm{rads}} - \dot{q}''_{\mathrm{loss}} \quad (29)$$

(3) Externally imposed radiant heat flux

When the external radiation penetrates the gas-soot mixture until it reaches the fuel surface, the radiative intensity is attenuated due to absorption of thermal energy by the soot-gas mixture. This attenuation of the radiation intensity can simply be described by the Bouguer's Law as follows:

$$\dot{q}''_{\mathrm{e}}(x) = \dot{q}''_{\mathrm{e}}(y) = \dot{q}''_{\mathrm{ext}}\mathrm{e}^{-\zeta(y)}. \quad (30)$$

Here $\dot{q}''_{\mathrm{ext}}$ is the externally incident radiant heat flux.

At the screen, y = 0 ($x = d$) and $\zeta(y = 0) = 0$, thus $\dot{q}''_e(x = d) = \dot{q}''_e(y = 0) = \dot{q}''_{\mathrm{ext}}$. While at the fuel surface, $y = d$ (x = 0) and $\zeta(y = d) = \zeta_d$, thus the "residue" external radiant flux that actually reaches the fuel surface can simply be obtained as

$$\dot{q}''_{\mathrm{es}} = \dot{q}''_{\mathrm{ext}}\mathrm{e}^{-\zeta_d}. \quad (31)$$

As the final result, substituting eqs. (27) and (30) into eq. (16), the net total radiative heat flux towards the fuel surface $\dot{q}''_R(x)$ can be derived. It is the universal source term of radiative energy in the energy conservation eq. (14), as a function of the temperature profile as well as optical thickness profiles which in turn depend on the temperature pro-

file and species distributions. Therefore, the whole problem can be solved by derivation of a numerical solution of the temperature profile from the energy conservation equation.

3.3 Extension of one-dimensional flame model to a small conical flame

In this study, the one-dimensional diffusion flame model is employed for evaluating heat transfer within the gas-soot mixture above the fuel surface and extending the understanding of heat transfer blockage occurring in small scale flames. Flame heat transfers are actually significantly affected by the geometrical features, especially radiative heat transfers. One-dimensional models provide the simplest geometry. In contrast, the flames in the FPA experiments are actually buoyant turbulent diffusion flames, which, for simplicity, are assumed and treated as cones of various heights having a fixed base. In order to reasonably compare analytical results with experimental data, it is necessary to build a "bridge" between the different flame geometries for reflecting inherent effect of flame geometry on the radiative heat transfer—extending application of the one-dimensional analysis to the conical flames.

For ideal conical flames having a same base, the flame height is the only key parameter to determine the flame geometry as the sample diameter is fixed in the experiments. For a buoyant turbulent diffusion flame, vertical gas velocities along the flame central line can be estimated as

$$\upsilon \propto \sqrt{gL}\,, \tag{32}$$

where L is the vertical distance above the fuel surface, g is the acceleration of gravity (9.8 m/s^2). Then the horizontal entrainment velocity of fresh "air" can be approximated as

$$\upsilon_e \approx \upsilon_0 \upsilon = \upsilon_0 \sqrt{gL}\,, \tag{33}$$

where the coefficient υ_0 is almost a constant. For an assumed conical flame, an element of flame surface area along L can be expressed as

$$\frac{dA_f}{dL} = \phi(Y_{o\infty})\pi\delta\left(1-\frac{L}{L_f}\right), \tag{34}$$

where A_f is the flame side surface area, L_f is the flame height, δ is the fuel surface diameter. $\phi = \phi(Y_{o\infty})$ is a flame shape parameter defined as the ratio of side areas of actual flames to conical flames, i.e.

$$\phi = \phi(Y_{o\infty}) = \frac{A_{f\_actual}}{A_{f\_conical}}. \tag{35}$$

The flame shape parameter ϕ denotes a deviation of actual flame shape from the assumed conical flame, as affected by ambient oxygen concentrations. $\phi = 1$ indicates a cone-shaped flame.

According to eqs. (33) and (34) the volumetric entrainment of "air" can be derived as

$$V_e = \int_0^{L_f} \upsilon_e \frac{dA_f}{dL} dL = \pi \upsilon_0 \delta \;\; \phi(Y_{o\infty})\sqrt{g}\int_0^{L_f} \sqrt{L}\left(1-\frac{L}{L_f}\right)dL$$

$$= \frac{4\pi}{15}\upsilon_0\delta \;\; \phi(Y_{o\infty})\sqrt{g}L_f^{3/2} = \frac{4\pi}{15}\upsilon_0\delta \;\; \phi(Y_{o\infty})\sqrt{g}L_f^{3/2}. \tag{36}$$

With the definition of oxygen to fuel stoichiometric mass ratio as

$$f = \frac{\dot{m}_{O_2}}{\dot{m}} = \nu_{O_2}\frac{M_{O_2}}{M_F}, \tag{37}$$

here M is the molecular weight of various species, ν_{O_2} represents mole number of oxygen needed for complete combustion of one mole fuel. For example f = 1.92 for PMMA. It is understood that the actual entrainment of oxygen would be up to 10 times of the stoichiometric mass ratio, i.e.

$$f_0 f = \frac{f_0\dot{m}_{O_2}}{\dot{m}} = \frac{V\rho_\infty Y_{o\infty}}{\pi\frac{\delta^2}{4}\chi_A\dot{m}''}. \tag{38}$$

Here the coefficient f_0 is a constant around 10. Also χ_A is the fraction of fuel that actually burns. Replacing V_e in eq. (38) with eq. (36) and solving the flame height yield

$$L_f = \left(\frac{15 f_0 f \chi_A \delta}{16\upsilon_0\sqrt{g}\rho_\infty Y_{o\infty}\phi(Y_{o\infty})}\right)^{2/3}\dot{m}''^{2/3}. \tag{39}$$

This is the relationship between the flame height and mass loss rate. The coefficient is a function of the ambient oxygen mass fraction $Y_{o\infty}$. In case that experimental data of both flame heights and fuel mass loss rates are available in this study, the coefficient can be determined by simplifying it as

$$\left(\frac{15 f_0 f \chi_A \delta}{16\upsilon_0\sqrt{g}\rho_\infty Y_{o\infty}\phi(Y_{o\infty})}\right)^{2/3} = \frac{a}{(1+bY_{o\infty})^{2/3}}. \tag{40}$$

Therefore the flame height can be derived as

$$L_f = \frac{a\dot{m}''^{2/3}}{(1+bY_{o\infty})^{2/3}}, \tag{41}$$

where a and b are constants determined by the experimental data of flame height and mass loss rate for best fitting.

For conical flames of a given height, the flame mean beam length and the view factor of radiative heat feedback from cone flame to the burning surface can easily be computed. Using these two important parameters that characterize the radiative features, application of the one-dimensional flame model is extended to the conical flames with following relationships:

(1) $$\frac{x_{cone}}{x_{one\text{-}dim}} = \frac{\ell_{cone}}{\ell_{one\text{-}dim}}, \tag{42}$$

where x is the one-dimensional coordinates specifying posi-

tions and ℓ is the mean beam length of flames [8]. Subscripts cone and one-dim represent conical or one-dimensional flame respectively.

(2) $$\dot{m}''\Delta H_{\mathrm{g}} = F\dot{q}''_{\mathrm{rads}} + \dot{q}''_{\mathrm{cons}} + \dot{q}''_{\mathrm{es}} - \dot{q}''_{\mathrm{loss}}. \quad (43)$$

This universal equation reveals the heat balance at the fuel surface, in which F is the newly introduced view factor. For one-dimensional flames, F = 1; for ideal cone-shaped flames, $F_{\mathrm{cone}} < 1$. All heat fluxes $\dot{q}''$ in this equation are computed from the one-dimensional model, the mass loss rate $\dot{m}''$ is then determined based on the different F. Definitions of ℓ_{cone}, $\ell_{\mathrm{one-dim}}$ and F_{cone} are given by eq. (33) and in Tables 1-4.2 and 1-4.1 of ref. [8] respectively.

For conical flames, based on the feature of volumetric absorption and emission of gas-soot mixtures, eq. (42) improves the optical and physical thicknesses of the conical volume from the one-dimensional volume, so that the radiative heat blockage and relevant parameters computed from the model are in an identical magnitude of cone-shaped volumes of gas-soot mixtures. While eq. (43) physically characterizes the radiative heat feedback of flames and the consequent mass loss rate based on the flame geometry. Therefore, the revised one-dimensional model is capable of analyzing the small scale FPA flames. Although these two equations are quite simple, detailed model studies have verified that the analytical results correspond well with the experimental data.

4 Result comparison and discussion

As stated above, eq. (8) has established a "bridge" for comparisons between theoretical predictions and experimental measurements. Figure 2 shows a comparison of the overall heat transfer blockage factor, plotting the model analytical results on the left hand side of the equation versus the experimental data on the right hand side of the equation. Each point in the figure represents an individual experiment under a given external radiant heat flux and ambient oxygen concentration.

In Figure 2, firstly, all the data points are located on or near the symmetric line, indicating a good agreement between the analytical and experimental results. Secondly, the higher the ambient oxygen concentration is, the larger the heat transfer blockage factors become. Thirdly, the heat transfer blockage factors for PMMA are slightly larger than those for POM under the same conditions. Additionally, all the analytical data of identical ambient oxygen concentrations under various external radiant heat fluxes between 10 and 60 kW/m^2 lies approximately along a horizontal line, implying that the predicted heat transfer blockage factors are independent of the external radiation. However, the same type of experimental data has a certain range of variation, this does not necessarily mean that the experimental heat transfer blockage factors vary as external radiation differs. The variation actually reflects errors in the linear slope measurements since a slight movement of an individual data point even within an acceptable accuracy would affect the overall linear slope.

Figure 3 shows the heat transfer blockage factor and its components β_{ext} and β_{int} of PMMA and POM flames as a function of the ambient oxygen concentrations. The experimental data is also given for comparison. The heat transfer blockage factor and its components increase as the ambient oxygen concentration rises.

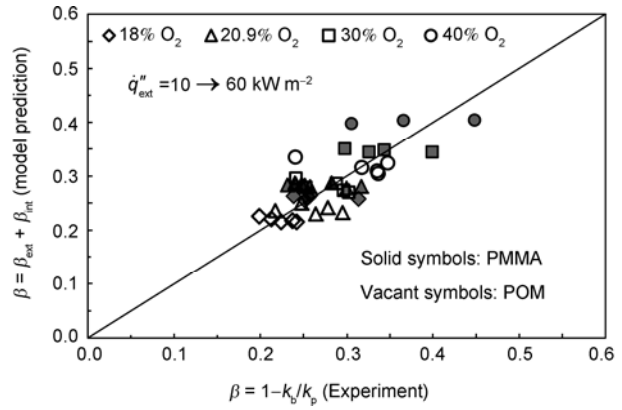

Figure 2 Comparisons between experimental and analytical heat transfer blockage factors.

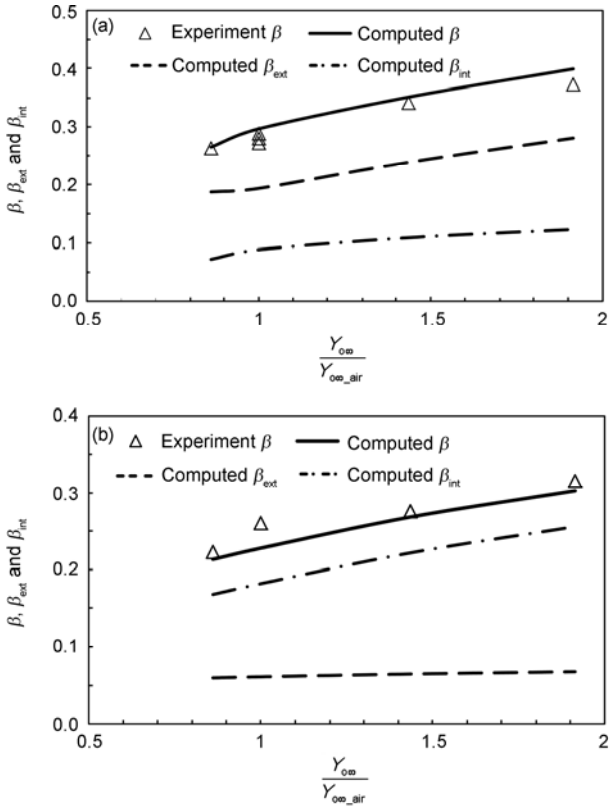

Figure 3 Effect of ambient oxygen concentration on blockage factors. (a) PMMA; (b) POM

Due to the different capability in absorption and emission, the two types of burning samples perform differently. PMMA flames are optically thicker, the blockage factor for the external radiation is the majority of the overall blockage factor. POM flames, on the contrary, are optically thinner having less thermal absorptions of the external radiation, as a result, the blockage factor for flame heat feedback β_{int} becomes the majority of the overall blockage factor. Because of the relatively weak radiation, convection is expected to be dominant in β_{int}.

Figure 4 illustrates the overall heat transfer blockage factor and its radiative and convective components (β_{rad} and β_{con}) of PMMA and POM flames, respectively. Superposition of the predicted data points of various external radiation further verifies that the blockage factor and its radiative and convective components are all independent of the external radiation. However, they increase as the ambient oxygen concentration rises.

Fundamentally, increase of the heat transfer blockage factors with the ambient oxygen fractions is due to the effect of both convective and radiative heat transfers. Both types of burning samples perform identically in the convective heat transfer blockage, as the ambient oxygen fraction rises, flame sheet temperature becomes higher, mass transfer at the fuel surface increases, cool fuel vapors lower the temperature near the surface, causing a more significant decrease of the convective heat feedback. However, both types of burning samples perform differently in the radiative heat transfer blockage, as the ambient oxygen fraction rises, PMMA flames have more soot and higher flame sheet temperature, so that become optically thicker absorbing more thermal energy. In contrast, POM flames have no soot, their optical thickness and radiative blockage factor are small and almost independent of the ambient oxygen fraction. Therefore, soot generation is considered as the primary driving force of the increased radiative blockage factor as the ambient oxygen fraction rises.

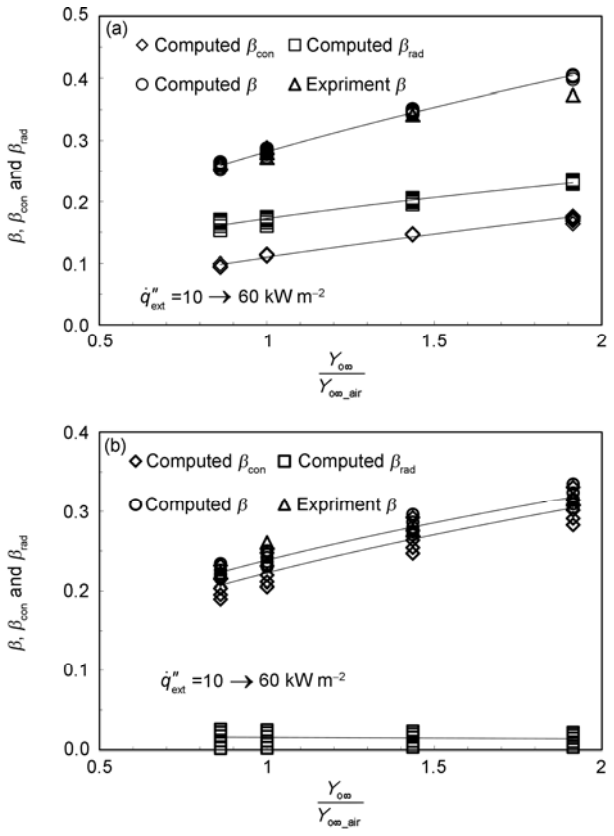

Figure 4 Heat transfer blockage factors as function of ambient oxygen fraction. (a) PMMA; (b) POM

Additionally, there is an obvious difference between PMMA and POM flames. For PMMA flames, radiative blockage is the majority of the overall heat transfer blockage; while for POM flames, the overall heat transfer blockage originates almost entirely from the convective blockage, the radiative blockage is nearly zero, implying that the invisibly light blue POM flames are nearly "transparent" to thermal radiation, i.e. as a result of absorption of thermal energy from the external radiation by the flame the increased flame radiative heat feedback can nearly compensate the attenuation of the external radiant heat flux.

Therefore, a certain convective blockage always exists in flames, since relatively cool fuel vapor convects heat away from the fuel surface. However, magnitude of the radiative blockage may vary significantly depending on flame absorptivity and emissivity. The radiative blockage factor β_{rad} defined in this study can be used to characterize the "transparency" of flames to thermal radiation, i.e. flames can be categorized as nearly transparent flame and non-transparent flame. According to the analytical results, PMMA has non-transparent flames, while POM has nearly transparent flames, in small scale combustion.

5 Conclusions

(1) Flame heat transfer blockage is a fundamental phenomenon in combustion of fires. However, it is difficult to carry out direct measurements, so few forceful experimental measurements are available at present. In this study, efforts have been made to develop an accurate measurement approach. With indirect measurement, eq. (8) not only defines the blockage factor of heat feedbacks to burning surface, but also provides an experimental understanding of the concept and quantity of the heat transfer blockage. In addition, it establishes a "bridge" for comparisons between analytical predictions and experimental measurements.

(2) It has been found from both the experimental and theoretical studies that the overall heat transfer blockage factors for PMMA and POM flames can be up to 0.4 and 0.3 respectively, and PMMA flames have somewhat larger blockage factors than POM. Furthermore, flame optical thicknesses and heat transfer blockage factors are almost independent of external radiation, but increase as the ambi-

ent oxygen concentration rises.

(3) In small scale combustion, gas absorption and emission are very important for evaluating flame radiation, especially for large amount of unburned fuel vapors near the burning surface that are sometimes strong absorbers and emitters. The PMMA and POM flames in the FPA experiment have demonstrated that gas radiation from small fires tends to be more prominent than soot radiation. Soot becomes increasingly important and soot generation is the primary driving force of the increased radiative blockage as the ambient oxygen concentration rises.

(4) Heat transfer blockage factors not only quantify magnitude of the heat transfer blockage, but also characterize the "transparency" of flames to thermal radiation. The newly defined radiative blockage factor has verified that PMMA flames are non-transparent while POM flames are nearly "transparent" in small scale combustion.

(5) The analytical results from the theoretical model are in a good agreement with the experimental data. The model studies have extended the conceptual and quantitative understandings of the flame heat transfer blockage phenomena.

1 de Ris J L, Fire radiation – A review. Proceedings of the Seventeenth Symposium (International) on Combustion. Pittsburgh: The Combustion Institute, 1979. 1003−1011

2 Jiang F H. Flame radiation from polymer fires. Fire Safety J, 1998, 30: 383−395

3 Hamins A, Fischer S J, Kashiwagi T, et al. Heat feedback to the fuel surface in pool fires. Combust Sci Technol, 1994, 97: 37−62

4 Tewarson A, Ogden S D. Fire behavior of polymethylmethacrylate. Combustion and Flame, 1992, 89: 237−259

5 Hopkins Jr D, Quintiere J G. Material fire properties and predictions for thermoplastics. Fire Safety J, 1996, 26: 241−268

6 Beaulieu P, Dembsey N A. Flammability characteristics at applied heat flux levels up to 200 kW/m^2. Fire Mater, 2007, 10: 1002

7 de Ris J L, Markstein G H, Orloff L, et al. Flame heat transfer Part I: Pyrolysis zone. Norwood, MA: FM Global Internal Technical Report, J.I. 0D0J9.MT, 2005

8 Tien C L, Lee K Y, Stretton A J. Radiation heat transfer. SFPE Handbook of Fire Protection Engineering. Quincy, MA: The National Fire Protection Association Press, 2002

9 Markstein G H. Measurements on gaseous-fuel pool fires with a fiber-optic absorption probe. Combust Sci Technol, 1984, 39: 215−233

10 Gregory J J, Keltner N R, Mata Jr R. Thermal measurements in large pool fires. Trans ASME, 1989, 111: 446−454

11 de Ris J L, Orloff L. Flame heat transfer between parallel panels. Proceedings of the Seventh Symposium (International) on Fire Safety Science. London: International Association of Fire Safety Science, 2006. 999−1010

12 Zhou Y P, Yang L Z, Dai J K, et al. Attenuation of incident heat flux by pyrolysis volatiles when heated using resistance element radiation heater. Fire Sci J, 2009, 27: 447−464

13 deRis J L, Markstein G H, Orloff L, et al. Similarity of turbulent wall fires. Proceedings of the Seventh Symposium (International) on Fire Safety Science. London: International Association of Fire Safety Science, 2005. 259−270

14 Park S H, Stretton A J, Tien C L. Infrared radiation properties of methyl methacrylate vapor. Combust Sci Technol, 1988, 62: 257−271

15 Wakatsuki K, Jackson G S, Hamins A, et al. Effects of fuel absorption on radiative heat transfer in methanol pool fires. Proceedings of the Thirty-First Symposium (International) on Combustion. Pittsburgh: The Combustion Institute, 2007. 2573−2580

16 Zhang H, Qi H Y, Lu Z A, et al. Influence of ventilation on the release of CO2 and CO in fire smoke (in Chinese). J Tsinghua Univ (Sci Technol), 2004, 44(8):1087−1091

17 Wang J T, Qi H Y, Li Y H, et al. Soot generation in combustion of hydrocarbon fuels (in Chinese). Proceedings of the Tenth Annual Conference. Chinese Society of Engineering Thermophysics, Qingdao, 2001. 463−468

18 Lou C, Chen C, Sun Y P, et al. Review of soot measurement in hydrocarbon-air flames. Sci China Ser E-Tech Sci, 2010, 53(8): 2129−2141

19 Wang Y, Yao Q, He X, et al. Electric field control of soot distribution in flames using laser-induced incandescence (in Chinese). Proc Chin Soc Elec Eng, 2008, 28(8): 34−39

20 Pagni P J, Okoh C I. Soot generation within radiating diffusion flames. Proceedings of the Twentieth Symposium (International) on Combustion. Pittsburgh: The Combustion Institute, 1984. 1045−1054

21 Staggs J E J. The heat of gasification of polymers. Fire Safety J, 2004, 39: 711−720

22 Tewarson A. Generation of heat and chemical compounds in fires. SFPE Handbook of Fire Protection Engineering. Quincy MA: The National Fire Protection Association Press, 2002

23 Beaulieu P A. Flammability characteristics at heat flux levels up to 200 kW/m^2 and the effect of oxygen in flame geat flux. Doctoral Dissertation. Worcester, US: Worcester Polytechnic Institute, 2005

24 Lee K Y, Zhong Z Y, Tien C L. Blockage of thermal radiation by the soot layer in combustion of condensed fuels. Proceedings of the Twentieth Symposium (International) on Combustion. Pittsburgh: The Combustion Institute, 1984. 1629−1636

25 Lee K Y, Tien C L. Radiation-induced ignition of condensed fuels in a ceiling fire including the effects of radiation blockage. Int J Heat Mass Transfer, 1986, 29(8): 1237−1244

26 Nicolette V F, Larson D W. The influence of large, cold objects on engulfing fire environments. Heat Mass Transfer Fires, 1990, 141: 63−71

27 Gritzo L A, Nicolette V F. Coupling of large fire phenomenon with object geometry and object thermal response. Fire Sci, 1997, 15: 427−442

28 Baek S W, Lee C. Heat transfer in a radiating medium between flame and fuel surface. Combustion and Flame, 1989, 75: 153−163

29 Chen S L, Ma H K, Chen D Y. Radiation blockage by the interaction of thermal radiation with conduction and convection in the combustion of condensed fuel. Int Comm Heat Mass Transfer, 1993, 20: 145−157

30 Bedir H, Tien J S. A computational study of flame radiation in PMMA diffusion flames including fuel vapor participation. Proceedings of the Twenty-Seventh Symposium (International) on Combustion. Pittsburgh: The Combustion Institute, 1998. 2821−2828

31 Jiang F H, de Ris J L, Qi H Y, et al. Radiation blockage in small scale PMMA combustion. Proceedings of the Thirty-third Symposium (International) on Combustion. Pittsburgh: The Combustion Institute, 2011. 2657–2664

32 Beier R A, Pagni P J. Soot volume fraction profiles in forced-combusting boundary layers. J Heat Transfer, 1983, 105: 159−165

33 Sparrow E M, Cess R D. Radiation Heat Transfer. Augmented ed. New York: McGraw Hill, 1978